arXiv:0710.5270v2 [cond-mat.stat-mech] 29 Jul 2009

Markov Properties of Electrical Discharge Current Fluctuations in Plasma

S. Kimiagar[1], M. Sadegh Movahed[2], S. Khorram [3] and M. Reza Rahimi Tabar[4,5]
[1] *Department of Physics,science faculty, Tehran central branch, Islamic Azad University, Tehran, Iran*
[2] *Department of Physics, Shahid Beheshti university, G.C., Evin, Tehran 19839, Iran*
[3] *Research Institute for Applied Physics and Astronomy, University of Tabriz, Tabriz 51664, Iran*
[4] *Department of Physics, Sharif University of Technology, P.O.Box 11365-9161, Tehran, Iran*
[5] *Carl von Ossietzky University, Institute of Physics, D-26111 Oldenburg, Germany*

Using the Markovian method, we study the stochastic nature of electrical discharge current fluctuations in plasma. Sinusoidal trends are extracted from the data set by the Fourier-Detrended Fluctuation analysis and consequently cleaned data is retrieved. We determine the Markov time scale of the detrended data set and show that it is almost a monotonic increasing function of discharge current intensity. We also estimate the Kramers-Moyal's coefficients of the discharge current and derive the corresponding Fokker-Planck equation. The obtained Langevin equation enables us to reconstruct discharge time series with similar statistical properties compared with the observed in the experiment. Finally the multifractal behavior of reconstructed time series using its Keramers-Moyal's coefficients and original data set are investigated.

I. INTRODUCTION

Many natural phenomena are identified by a degree of stochasticity. Turbulent flows, seismic recordings and plasma fluid are but a few examples of such phenomena [1–28]. Recently a robust statistical method has been developed to explore an effective equation that can reproduce stochastic data with an accuracy comparable to the measured one [18,19,29–34]. As in many early researches has been confirmed, one may utilize it to:
1 : reconstruct the original process with similar statistical properties, and
2 : understand the nature and properties of the stochastic process [18–22,29,30].

Interpretation and estimation of physical and chemical properties of plasma fluid have been one of the main research areas in the science of electromagnetic hydrodynamics. Fluctuations of electric and magnetic fields of plasma, spectral density, logistic mapping and nonlinearity of ionization wave have been investigated in Refs. [10–17,35–37]. It is well-known that discharge fluctuations in the plasma often exhibits irregular and complex behavior.

As we discussed in Ref. [17], because of some limitations in the experimental setup and data acquisition methods the measured plasma fluctuations may be affected by some trends such as; alternative power current oscillation, noise due to the electronic instruments and also fluctuations of striation areas near the anode and cathode plates. Consequently, inferring the reliable statistical properties of original fluctuations and to avoid spurious detection of correlations need to apply robust methods. Data set used through this paper were collected by a positive column of a hot cathode discharge in helium plasma. Details of our experimental setup is given in Ref. [17]. Cleaned data were constructed by applying the Fourier-Detrended Fluctuation analysis. Figure 1 shows typical detrended discharge current fluctuation. The size of recorded data points in each sampling is about 10^6.

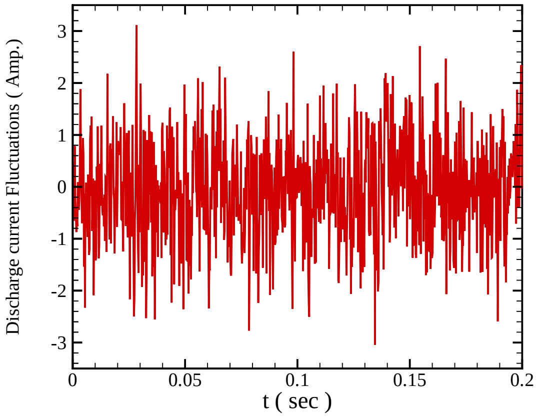

FIG. 1. Typical detrended electrical discharge current fluctuations in the plasma as a function of time.

Here using the Makovian method, we explore the statistical properties of discharge current fluctuations. We show that this approach will profoundly gives deep insight through the electromagnetic and hydrodynamics of discharge current in the ionized fluid. By addressing the implications dictated in [18,19] a Fokker-Planck evolution operator and Langevin equation will be found.

The rest of this paper is organized as follows: Section II is devoted to a brief summary of the most important notions and theorems on Markovian method and their application to the analysis of empirical data. Using the like-

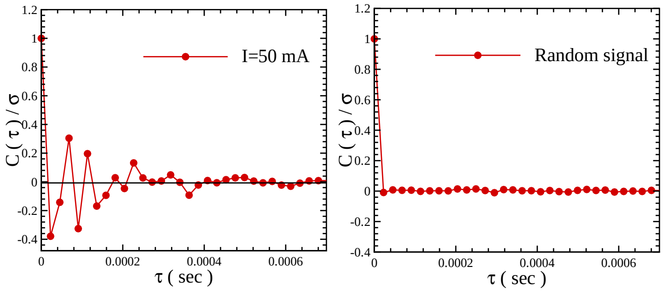

FIG. 2. Normalized correlation function for plasma cleaned data for discharge current with $I = 50\text{mA}$ (left panel) and for completely random data (right panel)

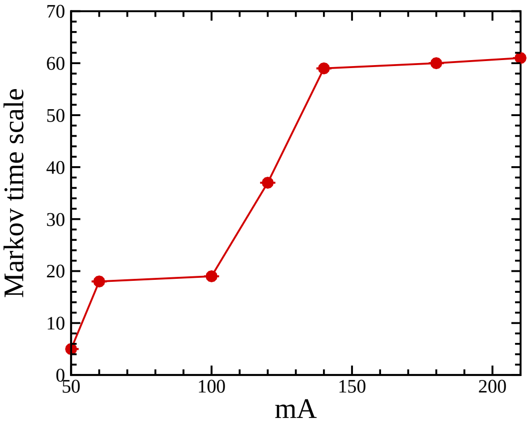

FIG. 3. Markov time scale as a function of discharge current intensity. The unit of vertical axis is $sec/44100$.

lihood statistics, we determined Markov time scale. Section III contains the main results of our analysis and estimate the Fokker-Planck and Langevin equations which govern the probability density function and stochastic variable (discharge current), respectively. Comparison between statistical and multifractal properties of original and reconstructed time series are also given in Section III. Section IV closes with a discussion and conclusion of the present results.

II. MARKOVIAN NATURE OF DATA SET

Let us begin with one of the simplest and most important statistical quantity of a given time series, that is the correlation function, which is written as

$$\mathcal{C}(X_1(t_1), X_2(t_2)) = \langle X_1(t_1) X_2(t_2) \rangle \tag{1}$$

here the sign $\langle . \rangle$, shows the ensemble averaging. We have set the average of time series equal to zero. For stationary time series the correlation function depends on only the separation time scale, which means that

$$\begin{aligned} \mathcal{C}(\tau) &\equiv \mathcal{C}(X_1(t_1), X_2(t_2)) \\ &= \langle X_1(t_1) X_2(t_1 + \tau) \rangle. \end{aligned} \tag{2}$$

In the presence of any trends and nonstationarity, correlation function depends not only to the time separation $(t_2 - t_1)$, but also to the starting and finishing times, namely t_1 and t_2, respectively. As demonstrated in Ref [17], the underlying detrended data for discharge current behaves as a stationary signal. The correlation function for plasma detrended data with $I = 50\text{mA}$ is plotted in the left hand side of the Figure 2. This figure confirms the underlying data sets behave as an anti-correlated series which has been observed in [17] using another method. We also present the same plot for a pure random signal, i.e. with Hurst exponent $H = 0.5$, in the right hand side of the Figure 2 for comparison.

As mentioned in introduction, here we use the Markovian method to explore the nature of stochasticity of discharge current fluctuations in plasma. To investigate the markovian nature of data, we briefly summarize the notions and theorems which will be importance for our statistical analysis of cleaned data set. For further details on Markov processes we refer the reader to the references [33,38–42].

Represent the discharge current fluctuations as a function of time by $X(t)$ and define $x(t) = X(t)/\sigma$, where σ is the standard deviation of discharge current fluctuations. Fundamental quantities related to the Markov processes are conditional probability density functions. The conditional probability density function (CPDF), $p(x_2, t_2|x_1, t_1)$, is defined as

$$p(x_2, t_2|x_1, t_1) = \frac{p(x_2, t_2; x_1, t_1)}{p(x_1, t_1)} \tag{3}$$

where $p(x_2, t_2; x_1, t_1)$ is the joint probability density function (JPDF), describing the probability of finding simultaneously, x_1 at scale(time), t_1, and x_2 at scale(time), t_2. Higher order conditional probability densities can be defined in an analogous way

$$p(x_N, t_N|x_{N-1}, t_{N-1}; ...; x_1, t_1) = \frac{p(x_N, t_N; ...; x_1, t_1)}{p(x_{N-1}, t_{N-1}; ...; x_1, t_1)} \tag{4}$$

where $p(x_N, t_N; x_{N-1}, t_{N-1}; ...; x_1, t_1)$ is N-point joint probability density function. Intuitively, the physical interpretation of a Markov process is that it "forgets its past," or, in other words, only the most nearby conditioning, namely x_{N-1} at t_{N-1}, is relevant to the probability of finding a fluctuation x_N at t_N. Hence, in the Markov process the ability to predict the value of x_N will not be enhanced by knowing its values in the steps prior to the most recent one. So an important simplification that is made for a Markov process is that, the conditional multivariate joint PDF is written in terms of the products of simple two parameter conditional PDF's [38] as

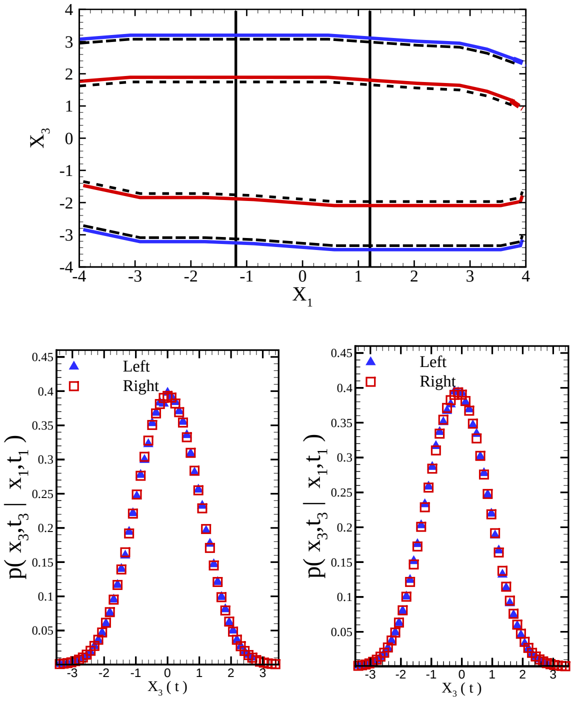

FIG. 4. Upper panel shows contour plots of the conditional PDF, $p(x_3,t_3|x_1,t_1)$. The solid and dashed line correspond to the left and right hand side of Eq. (11) for $t_3-t_1=2\times t_{\rm Markov}$, respectively. Inner contours are a cutting of PDF at 0.08 level and outer contours correspond to 0.005 level. Lower panel corresponds to the cuts through the conditional PDF for $x_1=\pm1.25\sigma$.

$$p(x_N,t_N;x_{N-1},t_{N-1};\cdots;x_2,t_2|x_1,t_1)$$

$$=\prod_{i=2}^{N}p(x_i,t_i|x_{i-1},t_{i-1}) \qquad (5)$$

To investigate whether underlying signal is a Markov process, one should tests the Eq. (5). But in practice for large values of N, is beyond the current computational capability. For $N=3$ (three points or events), however, the condition will be

$$p(x_3,t_3|x_2,t_2;x_1,t_1)=p(x_3,t_3|x_2,t_2) \qquad (6)$$

which should hold for any value of t_2 in the interval $t_1<t_2<t_3$. A process is then Markovian if the Eq. (6) is satisfied for a *certain* time separation t_3-t_2, in which case, we define the Markov time scale as $t_{\rm Markov}=t_3-t_2$. For simplicity, we let $t_2-t_1=t_3-t_2$. Thus, to compute the $t_{\rm Markov}$ we use a fundamental theory of probability according to which we write any three-point PDF in terms of the conditional probability functions as

$$p(x_3,t_3;x_2,t_2;x_1,t_1)$$

$$=p(x_3,t_3|x_2,t_2;x_1,t_1)p(x_2,t_2;x_1,t_1) \qquad (7)$$

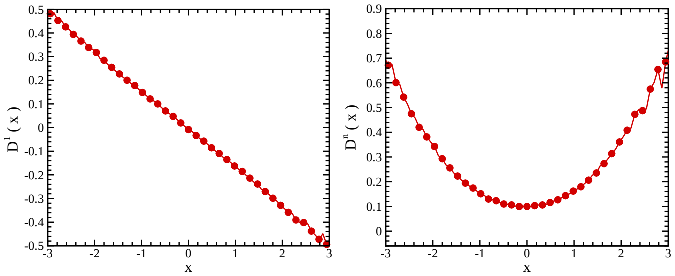

FIG. 5. Drift, $D^{(1)}(x)$, diffusion and $D^{(2)}(x)$ coefficients for data set with $I=50$mA.

Using the properties of Markov processes to substitute Eq. (7), we obtain

$$p_{\rm Mar}(x_3,t_3;x_2,t_2;x_1,t_1)$$

$$=p(x_3,t_3|x_2,t_2)p(x_2,t_2;x_1,t_1) \qquad (8)$$

In order to check the condition for the data being a Markov process, we must compute the three-point JPDF through Eq. (7) and compare the result with Eq. (8). The first step in this direction is determining the quality of the fit through the least-squared fitting quantity χ^2 defined by [4]

$$\chi^2=\int dx_1dx_2dx_3[p(x_3,t_3;x_2,t_2;x_1,t_1)$$

$$-p_{\rm Mar}(x_3,t_3;x_2,t_2;x_1,t_1)]^2/\left[\sigma^2_{3-{\rm joint}}+\sigma^2_{\rm Mar}\right] \qquad (9)$$

where $\sigma^2_{3-{\rm joint}}$ and $\sigma^2_{\rm Mar}$ are the variances of $p(x_3,t_3;x_2,t_2;x_1,t_1)$ and $p_{\rm Mar}(x_3,t_3;x_2,t_2;x_1,t_1)$, respectively. To compute the Markov time scale, we use the Likelihood statistical analysis [43]. In the absence of a prior constraint, the probability of the set of three-points JPDF is given by a product of Gaussian functions

$$\mathcal{L}(t_3-t_2)=\prod_{x_1,x_2,x_3}\frac{1}{\sqrt{2\pi(\sigma^2_{3-{\rm joint}}+\sigma^2_{\rm Mar})}}$$

$$\exp\left(-\frac{[p(x_3,t_3;x_2,t_2;x_1,t_1)-p_{\rm Mar}(x_3,t_3;x_2,t_2;x_1,t_1)]^2}{2(\sigma^2_{3-{\rm joint}}+\sigma^2_{\rm Mar})}\right) \qquad (10)$$

This probability distribution must be normalized. Evidently, when, for a set of values of the parameters, the χ^2 is minimum, the probability is maximum. The minimum value of χ^2_ν ($\chi^2_\nu=\chi^2/\mathcal{N}$, with $\mathcal{N}$ being the number of degree of freedom) corresponds to $t_{\rm Markov}$ for different value of electrical discharge current intensities. The values of Markov time scales, $t_{\rm Markov}$ in terms of discharge current intensity have been plotted in Figure 3. It must be pointed out that, the unit of $t_{\rm Markov}$ can be changed to the units of Seconds, using the rate of digitalization

TABLE I. The values of Kramers-Moyal coefficients for data set at different discharge current intensities.

	$D^{(1)}(x)$	$D^{(2)}(x)$
50mA	$-0.160\ x$	$0.090 + 0.003\ x + 0.070\ x^2$
60mA	$-0.058\ x$	$0.026 + 0.002\ x + 0.030\ x^2$
100mA	$-0.052\ x$	$0.026 + 0.002\ x + 0.026\ x^2$
120mA	$-0.028\ x$	$0.013 + 0.001\ x + 0.014\ x^2$
140mA	$-0.017\ x$	$0.008 + 0.001\ x + 0.009\ x^2$
180mA	$-0.017\ x$	$0.008 + 0.001\ x + 0.009\ x^2$
210mA	$-0.016\ x$	$0.009 + 0.001\ x + 0.008\ x^2$

in the experimental setup, 44100 *sample/sec* (for simplification we use "sec" as an abbreviation of "second" for unit of time in whole of paper).

One can write Eq. (8) as an integral equation, which is well-known as the Chapman-Kolmogorov (CK) equation

$$p(x_3,t_3|x_1,t_1) = \int dx_2\ p(x_3,t_3|x_2,t_2)\ p(x_2,t_2|x_1,x_1) \tag{11}$$

We have checked the validity of the CK equation for describing the time scale separation of t_1 and t_2 being equal to the Markov time scale. This is shown in Figure 4 (for the data set with electrical current intensity, $I = 50$ mA). In this figure, the upper panel shows the contour plot of identification of the left (solid line) and right (dashed line) sides of Eq. (11) for two levels, 0.080 (inner contour) and 0.005 (outer contour). The conditional PDF $p(x_3,t_3|x_1,t_1)$, for $x_1 = \pm1.25\sigma$, are shown in the lower panel. All the scales are measured in unit of the standard deviation of the discharge current fluctuations. We must point out that if all situations to be same as our experimental setup such as pressure, current intensity and so on, one can expect that all values derived by Markov analysis would be repeated. The value of Markov time scale increases as discharge current intensity increases (see Figure 3). It seems that by increasing the current intensity, charges become more energetic, therefore their effective cross-section will decrease and hence increasing their memory.

Up to now we determined the Markov time scale for each cleaned data set over which time series behaves as a Markov process. In the next section we will turn to the deriving master and stochastic equations governing the evolution of probability density function and fluctuation itself, respectively.

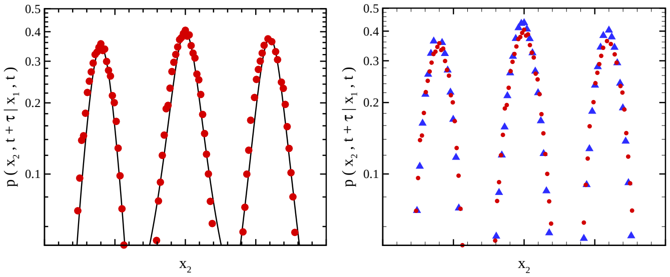

FIG. 6. Left panel corresponds to the conditional probability density function determined by analytical formula, Eq. (17) (solid line) and directly computed by original cleaned data (symbol) for $I = 50$mA. Right panel shows the comparison between the conditional probability density function determined by generated data using Eq. (16) (triangle symbol) and our initial cleaned data (circle symbol). In each panel, the plots from left to right correspond to the cut for $x_1 = -0.5\sigma$, $x_1 = 0.0$ and $x_1 = +0.5\sigma$ level, respectively. To make more obvious, we shifted the value of x_2 for each plot. We took $\tau = t_{\mathrm{Markov}}$, where t_{Markov} is the Markov time scale of data set.

III. LANGEVIN EQUATION: EVOLUTION EQUATION TO DESCRIBE THE PLASMA DISCHARGE CURRENT FLUCTUATIONS

The Markovian nature of the plasma electrical discharge fluctuations enables us to derive a Fokker-Planck equation - a truncated Kramers-Moyal equation - for the evolution of the PDF $p(x,t)$, in terms of time t. The Chapman-Kolmogorov (CK) equation, formulated in differential form, yields the following Kramers-Moyal (KM) expansion [38]

$$\frac{\partial}{\partial t}p(x,t) = \sum_{n=1}^{\infty}\left(-\frac{\partial}{\partial x}\right)^n [D^{(n)}(x,t)p(x,t)] \tag{12}$$

where $D^{(n)}(x,t)$ are called as the Kramers-Moyal's coefficients. These coefficients can be estimated directly from the moments, $M^{(n)}$, and the conditional probability distributions as

$$D^{(n)}(x,t) = \frac{1}{n!}\lim_{\Delta t\to 0} M^{(n)} \tag{13}$$

$$M^{(n)} = \frac{1}{\Delta t}\int dx'(x'-x)^n p(x',t+\Delta t|x,t) \tag{14}$$

For a general stochastic process, all Kramers-Moyal's coefficients are different from zero. According to Pawula's theorem, however, the Kramers-Moyal expansion stops after the second term, provided that the fourth order coefficient $D^{(4)}(x,t)$ vanishes. In that case, the Kramers-Moyal expansion reduces to a Fokker-Planck equation (also known as the backwards or second Kolmogorov equation) [38]

$$\frac{\partial}{\partial t}p(x,t) \; = \; \left\{-\frac{\partial}{\partial x}D^{(1)}(x,t) \, + \, \frac{\partial^2}{\partial x^2}D^{(2)}(x,t)\right\}p(x,t) \tag{15}$$

Also the evolution equation for conditional probability density function is given by the above equation except that $p(x,t)$ is replaced by $p(x,t|x_1,t_1)$. Here $D^{(1)}$ is known as the drift term and $D^{(2)}$ as diffusion term which represents the stochastic part. The Fokker-Planck equation describes the evolution of probability density function of a stochastic process generated by the Langevin equation (we use the Itô's definition) [38]

$$\frac{\partial}{\partial t}x(t) = D^{(1)}(x,t) + \sqrt{D^{(2)}(x,t)}f(t) \tag{16}$$

where $f(t)$ is a random force, i.e. δ-correlated white noise in t with zero mean and gaussian distribution, $\langle f(t)f(t')\rangle = 2\delta(t-t')$. Using Eqs. (13) and (14), for collected data sets, we calculate drift, $D^{(1)}$, and diffusion, $D^{(2)}$, coefficients, shown in Figure 5. It turns out that the drift coefficient $D^{(1)}$ is a linear function in t, whereas the diffusion coefficient $D^{(2)}$ is a quadratic function. For large values of x, our estimations become poor, the uncertainty increases, so we truncate our estimations up to 3σ of fluctuations as indicated in Figure 5.

The functional feature of drift and diffusion coefficients for different electrical discharge data sets are reported in Table I. To ensure that Kramers-Moyal expansion (Eq. (12)) reduces to a Fokker-Planck equation (Eq. (15)), we compute fourth-order coefficient $D^{(4)}$. In our analysis, $D^{(4)} \simeq 10^{-1}D^{(2)}$. One must point out that, however the fourth-order Kramers-Moyal's coefficient is not so small, but in the current analysis, this doesn't make measurable uncertainty in our results (see below). Furthermore, using Eq. (16), it becomes clear that we are able to separate the deterministic and the noisy components of the fluctuations in terms of the coefficients $D^{(1)}$ and $D^{(2)}$. According to the values of the Kramers-Moyal's coefficients reported in Table I, it is possible to reconstruct discharge current fluctuations at arbitrary current intensity using Eqs. (15) and (16) [18].

Now let us have a comparison of the statistical properties of reconstructed data using Eq. (16) with the original fluctuations. For this purpose, we rely on the solution of Fokker-Planck equation for conditional probability function (same as Eq. (15) for infinitesimally small step τ) which is given by [38]

$$p(x_2,t+\tau|x_1,t) = \frac{1}{2\sqrt{\pi D^{(2)}(x_2,t)\tau}} \times \exp\left(-\frac{(x_2-x_1-D^{(1)}(x_2,t)\tau)^2}{4D^{(2)}(x_2,t)\tau}\right) \tag{17}$$

Left panel of Figure 6 shows conditional probability density function computed by the above equation and directly calculated from the original detrended data set for $I = 50$mA. The plot from left to right correspond to $x_1 = -0.5\sigma$, $x_1 = 0.0$ and $x_1 = +0.5\sigma$ level, respectively. We also compute the conditional probability using reconstructed fluctuations via Eq. (16) and compare it with the same one for original cleaned data at three mentioned levels for x_1. We took $\tau = t_{\rm Markov}$ for all plots in Figure 6.

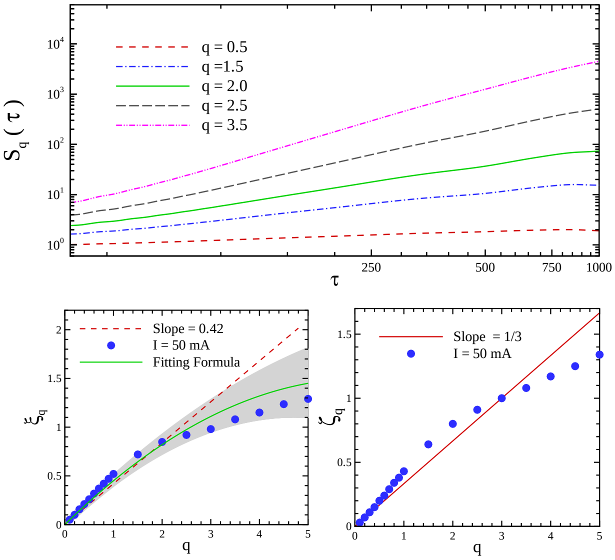

FIG. 7. Upper panel indicates the structure function versus τ. Lower left panel shows the scaling exponent of $S_q(\tau)$ as a function of moment for original cleaned plasma fluctuations (filled symbol) and solid line corresponds to the fitting formula derived by Kramers-Moyal's coefficients for multi-fractal anti-correlated signal with $H = 0.42$ (see Eq. (27)). Also in this panel, dashed line corresponds to a mono-fractal anti-correlated series. Lower right panel indicates $\zeta(q)$ versus q. Here we chose the data set with $I = 50$mA.

To check the multifractal nature of reconstructed time series, we investigate the Markovian nature of the increments which is defined as: $\Delta x(\tau) = x(t+\tau) - x(t)$. According to the mentioned procedure, we can determine the Markov time scales for the increments and calculate the Kramers-Moyal's coefficients. Likelihood analysis confirms that, the increment signal of plasma fluctuations for all electrical current intensities are also Markov processes. The Fokker-Planck equation for probability density function of the increment is given by [44,45]

$$-\tau\frac{\partial}{\partial\tau}p(\Delta x,\tau) = \left\{-\frac{\partial}{\partial\Delta x}D^{(1)}(\Delta x,\tau) + \frac{\partial^2}{\partial\Delta x^2}D^{(2)}(\Delta x,\tau)\right\}p(\Delta x,\tau) \tag{18}$$

the negative sign of the left-hand side of Eq. (18) is due to the direction of the cascade from large to smaller time scales τ. The corresponding Langevin equation can be read as

$$-\tau\frac{\partial}{\partial\tau}\Delta x(\tau) = D^{(1)}(\Delta x,\tau) + \sqrt{D^{(2)}(\Delta x,\tau)}f(\tau) \quad (19)$$

where $f(\tau)$ is the same as random function in equation 16. For time series with scaling correlations the Drift and diffusion coefficients of increment are formulated as [44–46]

$$\begin{aligned} D^{(1)}(\Delta x,\tau) &\simeq -H\Delta x \\ D^{(2)}(\Delta x,\tau) &\simeq b\Delta x^2 \end{aligned} \quad (20)$$

Using Eqs. (18) and (20) we obtain the evolution of structure functions ($S_q(\tau) \equiv \langle|\Delta x(\tau)|^q\rangle = \langle|x(t+\tau) - x(t)|^q\rangle$) as follows

$$\begin{aligned} -\tau\frac{\partial}{\partial\tau}\langle|\Delta x(\tau)|^q\rangle &= q\langle|\Delta x(\tau)|^{q-1}D^{(1)}(\Delta x,\tau)\rangle \\ &+q(q-1)\langle|\Delta x(\tau)|^{q-2}D^{(2)}(\Delta x,\tau)\rangle \end{aligned} \quad (21)$$

by substituting the Eqs. (20) in Eq. (21) we find

$$\tau\frac{\partial}{\partial\tau}\langle|\Delta x(\tau)|^q\rangle = [qH - bq(q-1)]\langle|\Delta x(\tau)|^q\rangle \quad (22)$$

the above equation implies scaling behavior for moments of increments, structure function as

$$S_q(\tau) \equiv \langle|\Delta x(\tau)|^q\rangle = \langle|x(t+\tau) - x(t)|^q\rangle \sim \tau^{\xi(q)} \quad (23)$$

According to Eqs. (22) and (23), the corresponding scaling exponent in general case can be read as

$$\xi(q) = qH - bq(q-1) \quad (24)$$

For mono- and multi-fractal processes the exponent $\xi(q)$ have linear and non-linear behavior with q, respectively. It must point out that H is nothing except the underlying fluctuations's Hurst exponent [47–50]. To check the estimated scaling exponent $\xi(q)$ (Eq. (24)) with original time series we use the extended self similarity (ESS) method [51,52]. In the ESS method, the log-log plot of $S_q(\tau)$ as a function of specific order of structure function, namely $S_3(\tau)$, usually shows an extended scaling regime

$$S_q(\tau) \sim S_3(\tau)^{\zeta(q)} \quad (25)$$

For any Gaussian process, the exponent in the above equation is given by $\zeta(q) = q/3$ [51,52]. Any deviation from this relation can be interpreted as a deviation from Gaussianity. Figure 7 shows the log-log plot of structure function in terms of time scaling (upper panel), exponents $\xi(q)$ (left lower panel) and $\zeta(q)$ (right lower panel) for the plasma fluctuations with $I = 50$mA. The present results are in agrement with our previous results derived that the plasma time series have multi-fractal nature [17].

TABLE II. The values of moments, $\langle x^n\rangle$, and their errors for data set at different discharge current intensities.

	$\langle x^2\rangle \times 10^{+5}$	$\langle x^3\rangle \times 10^{+9}$	$\langle x^4\rangle \times 10^{+9}$
50mA	2.483 ± 0.001	-0.395 ± 0.417	1.842 ± 0.062
60mA	2.415 ± 0.001	-3.330 ± 0.123	1.532 ± 0.001
100mA	2.879 ± 0.001	-17.500 ± 1.990	4.140 ± 0.318
120mA	2.600 ± 0.001	-3.140 ± 0.179	1.858 ± 0.008
140mA	2.095 ± 0.001	-5.770 ± 0.380	1.431 ± 0.030
180mA	1.617 ± 0.001	-7.220 ± 2.850	2.002 ± 0.765
210mA	1.383 ± 0.001	-0.458 ± 0.139	0.811 ± 0.335

The obtained expression for $D^{(1)}(\Delta x,\tau)$ and $D^{(2)}(\Delta x,\tau)$ (to avoid the overissue we just report the results of data for $I = 50$mA) are as follows

$$\begin{aligned} D^{(1)}(\Delta x,\tau) &= -(0.45 \pm 0.03)\Delta x \\ D^{(2)}(\Delta x,\tau) &= (0.04 \pm 0.01)\Delta x^2 \end{aligned} \quad (26)$$

consequently, using Eqs. (26) and (24), the scaling exponent is determined as

$$\xi(q) = (0.45 \pm 0.03)q - (0.04 \pm 0.01)q(q-1) \quad (27)$$

As shown in the lower left panel of Figure 7, the above function for $\xi(q)$ (solid line) with the shaded area corresponds to 68.3% confidence interval derived by Markovian analysis of increments has an acceptable confidence level to experimental results (filled symbol).

Finally we check the Gaussian nature of the PDFs of reconstructed and detrended time series. For a Gaussian distribution, all the even moments are related to the second moment through $\langle x^{2n}\rangle = \frac{2n!}{2^n n!}\langle x^2\rangle^n$ (e.g., for $n = 2$, $\langle x^4\rangle = 3\langle x^2\rangle^2$), while the odd moments are zero identically. We can directly check the relation between the higher moments for the plasma fluctuations data at different value of discharge current intensities with second moment. The values of moments and their variances calculating directly from data are summarized in Table II.

Let us examine the predictions for the moments of the plasma fluctuations via the Fokker-Planck equation, and compare their values with the direct evaluation represented in Table II. Using the general Kramers-Moyal expansion, Eq. (12), which is also valid for the probability density $p(x,t)$, differential equations for the n-th order moments can be derived. By multiplication of the both side of Eq. (12) with x^n and integration with respect to x, we can obtain evolution of different moments of data set as

$$\frac{d}{dt}\langle x^n(t)\rangle = \sum_{k=1}^{\infty}(-1)^k\int_{-\infty}^{+\infty} x^n\left(\frac{\partial}{\partial x}\right)^k D^{(k)}(x,t)p(x,t)dx$$

$$= \sum_{k=1}^{n} \frac{n!}{(n-k)!} \int_{-\infty}^{+\infty} x^{n-k}\, D^{(k)}(x,t)\, p(x,t) dx$$
$$= \sum_{k=1}^{n} \frac{n!}{(n-k!)} \left\langle x^{n-k}\, D^{(k)}(x,t) \right\rangle \qquad (28)$$

We put $n = 4$ in the above equation and find the equation for the fourth moment as follows

$$\frac{d}{dt}\langle x^4(t)\rangle = 4\langle D^{(1)}(x)x^3(t)\rangle + 12\langle D^{(2)}(x)x^2(t)\rangle$$
$$+24\langle D^{(3)}(x)x(t)\rangle + 24\langle D^{(4)}(x)\rangle. \qquad (29)$$

The third and fourth Kramers-Moyal's coefficients for the data set are reported in Table III. We should point out that the values of $|D^{(3)}|$ and $|D^{(4)}|$ are less than $|D^{(2)}|$. For the stationary case, all the moments of fluctuations are time independent and the left-hand side of Eq. (29) vanishes, so

$$\langle x^4\rangle = [\alpha_2(I) \pm \sigma_2(I)]\langle x^2\rangle^2 + [\alpha_3(I) \pm \sigma_3(I)]\langle x^3\rangle\sqrt{\langle x^2\rangle} \qquad (30)$$

where $\alpha_2(I)$ determines the coefficient of Kurtosis quantity and $\sigma_2(I)$ shows its variance. Also $\alpha_3(I)$ determines the coefficient of Skewness and $\sigma_3(I)$ indicates its error. Skewness measures the asymmetry of probability density function and Kurtosis determines the statistic of rare events in the processes. In generally they may depend to the discharge current intensity, I. Using the results represented in Table III, for each case of fluctuations $\alpha_n(I)$ and its variance are given in Table IV.

As we mentioned before, for exact Gaussian process, we should have

$$\alpha_2(I) = \frac{\langle x^4\rangle}{\langle x^2\rangle^2} = 3.0 \qquad (31)$$
$$\alpha_3(I) = 0.0 \qquad (32)$$

If $\alpha_2(I) > 3.0$ means that probability density function has fat tail and rare events have more chance to occur. While for $\alpha_2(I) < 3.0$, the tails of probability density function is heavy than the Gaussian distribution. According to the values of $\alpha_2(I)$ and $\alpha_3(I)$, we find that probability density function of data set is deviated from Gaussian.

TABLE III. The values of third and fourth Kramers-Moyal coefficients for data set at different discharge current intensities.

	$D^{(3)}(x)$	$D^{(4)}(x)$
50mA	$-0.007 - 0.073\,x$ $-0.019\,x^3$	$0.009 + 0.009\,x + 0.010\,x^2$ $-0.001\,x^3 + 0.001\,x^4$
60mA	$-0.024\,x - 0.002\,x^2$ $-0.010\,x^3$	$0.001 - 0.020\,x + 0.010\,x^2$ $+0.001\,x^3 + 0.003\,x^4$
100mA	$-0.025\,x - 0.001\,x^2$ $-0.009\,x^3$	$0.002 + 0.001\,x + 0.013\,x^2$ $+0.002\,x^4$
120mA	$-0.013\,x - 0.005\,x^3$	$0.001 + 0.006\,x^2 + 0.001\,x^4$
140mA	$-0.008\,x - 0.003\,x^3$	$0.0009 + 0.003\,x^2 + 0.001\,x^4$
180mA	$-0.007\,x - 0.003\,x^3$	$0.0007 + 0.002\,x^2 + 0.001\,x^4$
210mA	$-0.009\,x - 0.002\,x^3$	$0.0008 + 0.005\,x^2$

IV. SUMMARY AND CONCLUSION

We have studied the stochastic nature of the electrical discharge current fluctuations in the Helium plasma as a working gas. Due to the sinusoidal trend we should distinguish the intrinsic fluctuations from nonstationarity to infer valuable statistical properties of data set. Therefore for every stochastic analysis to avoid detection of spurious statistical properties we had to first clean the data set, then apply the statistical method to analysis the signal. We have applied the Fourier-Detrended Fluctuations Analysis method to extract sinusoidal trend.

We showed that how the mathematical framework of Markov processes can be applied to develop a successful statistical description of the plasma fluctuations. We have analyzed detrended data via Markovian method. The Markov time scale, as the characteristic time scale of the Markov properties of the electrical discharge current fluctuations, was obtained. According to the theory of the stochastic process, the electrical discharge current at time scales larger than the Markov time scale can be considered as a Markov process. This means that the data located at the separations larger than the Markov time scale can be described as a Markov chain. It is found that Markov time scale, t_{Markov} increases by increasing the current intensity in the plasma. This means that the memory of charged particles in the plasma increase as current intensity increases. It is due to the fact that particles become more energetic, therefore they can penetrate deeper in the plasma without considerable deviation from the initial way. Then every new situation keeps the memory of some nearby conditioning corresponds to its

TABLE IV. The values of α's coefficients and their variances, σ's, for data set at different discharge current intensities.

	α_2	σ_2	α_3	σ_3
50mA	3.14	0.38	0.18	0.21
60mA	3.81	0.70	−1.17	0.51
100mA	2.86	0.53	−3.68	0.66
120mA	2.77	0.98	2.25	0.96
140mA	3.05	0.56	−2.09	0.35
180mA	3.67	0.85	−0.01	0.28
210mA	3.08	0.95	−4.18	0.95

Markov time scale. In other words by increasing the current intensity, effective scattering cross-section decreases so mean free time increases [53] as well as corresponding Markov time scale. According to the Markovian nature of fluctuations, we demonstrated that, the probability density function of fluctuations satisfies a Fokker-Planck equation. The Langevin equation, governing the evolution of current fluctuations also has been given.

To check the multifractality nature of the time series, we used the scaling properties of structure function and concept of Extended-Self-Similarity [54,55]. By computing the corresponding Kramers-Moyal's coefficients, we find a good consistency between multifractality nature of original time series and the obtained exponents from the reconstructed Fokker-Planck equation.

Acknowledgements Authors would like to thank S. Sobhanian for useful comments and discussions.

---

[1] S. Torquato, *Random Heterogeneous Materials* (Springer, New York, 2002); C.L.Y. Yeong and S. Torquato, Phys. Rev. E **57**, 495 (1998); *ibid.* **58**, 224 (1998).
[2] M. Sahimi, *Heterogeneous Materials*, Volume II (Springer, New York, 2003).
[3] D. N. Spergel, L. Verde, H. V. Peiris, E. Komatsu, M. R. Nolta, C. L. Bennett, M. Halpern, G. Hinshaw, N. Jarosik, A. Kogut, M. Limon, S. S. Meyer, L. Page, G. S. Tucker, J. L. Weiland, E. Wollack, E. L. Wright, Astrophys.J.Suppl. **148** , 175 (2003).
[4] F. Ghasemi, A. Bahraminasab, M. Sadegh Movahed, S. Rahvar, K. R. Sreenivasan and M. Rahimi Tabar, J. Stat. Mech. P11008 (2006).
[5] M. Sadegh Movahed, F. Ghasemi, S. Rahvar and M. Rahimi Tabar, arXiv:astro-ph/0602461.
[6] G. R. Jafari, M. S. Movahed, S. M. Fazeli, M. Reza Rahimi Tabar, S. F. Masoudi, J. Stat. Mech. P06008 (2006).
[7] G. R. Jafari, M. Sadegh Movahed, P. Noroozzadeh, A. Bahraminasab, Muhammad Sahimi, F. Ghasemi, M. Reza Rahimi Tabar, International Journal of Modern Physics C Vol. 18, No. 11, 16891697(2007).
[8] M. Sadegh Movahed and Evalds Hermanis, Journal of Physica A: Statistical Mechanics and its Applications, 387 915 (2008).
[9] M. Sadegh Movahed, G. R. Jafari, F. Ghasemi, S. Rahvar and M. Rahimi Tabar, J. Stat. Mech. P02003 (2006).
[10] A. Garscadden and K. G. Emeleus, Proc. Phys. Soc., **79** (1962).
[11] W. X. Ding, T. Klinger and A. Piel, Phys. Lett. A , **222** (1996).
[12] J. Qin, L. Wang, D. P. Yuan, P. Gao, and B. Z. Zhang, Phys. Rev. Lett., **63**, 163 (1989).
[13] Z. Donko and L. Szalia, Chaos, Solitons, Fractals, **7**, 5 (1996).
[14] T. Gyegyek, Plasma Phys. and Cont. Fusion, **41** (1999).
[15] C. Franck, T. Klinger and A. Piel, Phys. Lett.A, **259** (1999).
[16] C. Letellier, O. Menard, T. Klinger, A. Piel and G. Bonohomme, Physica D, **156** (2001).
[17] S. Kimiagar, M. Sadegh Movahed, S. Khorram, S. Sobhanian, and M. Reza Rahimi Tabar, J. Stat. Mech. P03020 (2009).
[18] G. R. Jafari, S. M. Fazeli, F. Ghasemi, S. M. Vaez Allaei, M. R. Tabar, A. Iraji Zad, and G. Kavei, Phys. Rev. Lett. **91**, 226101 (2003).
[19] M. Waechter, F. Riess, H. Kantz and J. Peinke, Europhysics Letters **5**, 579 (2003)
[20] M. Reza Rahimi Tabar, F. Ghasemi, J. Peinke, R. Friedrich, K. Kaviani, F. Taghavi, S. Sadeghi, G. Bijani and M. Sahimi,Computing In Scince and Engeering ,86, (2006).
[21] F. Ghasemi, J. Peinke, M. Sahimi, and M.R. Rahimi Tabar, European Physical J. B **47**, 411, 29 (2005).
[22] F. Ghasemi, J. Peinke M. Reza Rahimi Tabar and Muhammad Sahimi, to be published in Intl J. Modern Physics C, (2005).
[23] C. V. Chianca, A. Ticona and T. J. P. Penna, Physica A, **357**, 447 (2005).
[24] C. K. Peng ,S. V. Buldyrev ,S. Havlin ,M. Simons ,H. E. Stanley , and A. L. Goldberger , Phys. Rev. E **49**, 1685 (1994). ;S. M. Ossadnik ,S. B. Buldyrev ,A. L. Goldberger ,S. Havlin , R. N.Mantegna ,C. K. Peng , M. Simons and H. E. Stanley, Biophys. J. **67**, 64, (1994).
[25] J. W. Kantelhardt, E. Koscielny-Bunde, H. H. A. Rego, S. Havlin and A. Bunde, Physica A **295**, 441 (2001).
[26] Z. Chen, P. Ch. Ivanov, K. Hu and H. E. Stanley, Phys. Rev. E **65**, preprint physics/0111103 (2002).
[27] C. K. Peng, S. Havlin, H. E. Stanley and A. L. Goldberger, Chaos **5** 82 (1995).
[28] A. Bunde, S. Havlin, J. W. Kantelhardt, T. Penzel, J. H. Peter and K. Voigt, Phys. Rev. Lett. **85**, 3736 (2000).
[29] Siegert S., Friedricha R. and Peinke J., arXiv:cond-mat/9803250
[30] Christoph R., Peinke J. and Friedrich R. J. Fluid Mech. **433**, pp.383. (2001).
[31] R. Friedrich , J. Peinke Phys. Rev. Lett. **78**, 863 (1997).
[32] R. Friedrich ,J. Peinke and C. Renner Phys. Rev. Lett, **84**, 5224 (2000).
[33] R. Friedrich ,k. Marzinzik & Schmigel A. in *"A perspective Look at Nonlinear Media"*, Edited by Jurgen

Parisi,C. Stefan Muller and Walter Zimmermann, Lecture notes in Physics, Vol. **503**, P. 313 (Springer-verlag, Berlin, 1997).
[34] R. Friedrich ,C. Renner ,M. Siefert and J. Peinke Phys. Rev. Lett. **89**, 149401 (2002).
[35] F. Sigeneger and k. Winkler, Applied Physics, **19**, 211-223 (2002).
[36] A. V. Isupov and I. M. Ulanov, High Temprature, **43**, 169 (2005).
[37] I. Denysenko *et al*, Physics of Plasma, **13**073507 (2006).
[38] H. Risken, "*The Fokker-Planck equation*", (Springer-Verlag Berlin, 1984);N. G. Van Kampen, "*Stochastic processes in physics and chemistry*" (North Holland, Amsterdam, 1981);C.W. Gardiner, "*Handbook of Stochastic Methods*", (Springer-Verlag Berlin, 1983)
[39] P.Ḧanggi, and H. Thomas, Physics Reports **88**, 207 (1982).
[40] R. Friedrich, J. Peinke, and Ch. Renner, Phys. Rev. Lett., **84**, 5224 (2000).
[41] Ch. Rener, J. Peinke and R. Friedrich, JFM **433** , 383 (2001).
[42] Friedrich, R., Zeller J., and Peinke J., Europhys. Lett. **41**, 153 (1998).
[43] Jr. R.Colistete , J.C. Fabris, S. V. B. Goņcalves and P. E. de Souza , Int. J. Mod. Phys. **D** 13, 669
[44] R. Friedrich, J. Peinke and Ch. Renner, Phys. Rev. Lett., **84**, 5224 (2000).
[45] Ch. Renner, J. Peinke and R. Friedrich, arXiv:cond-mat/0102494
[46] M. Waechter, F. Riess, Th. Schimmel, U. Wendt and J. Peinke, The European Physical Journal B **41**, pp. 259 (2004).
[47] H. E. Hurst ,R. P. Black and Y .M. Simaika , "*Long-term storage. An experimental study*" (Constable, London 1965).
[48] A. Eke, P. Herman, L. Kocsis and L. R. Kozak, Physiol. Meas. **23**, R1, (2002).
[49] E. Koscielny-Bunde ,H. E. Roman ,A. Bunde ,S. Havlin and H. J. Schellnhuber , Phil. Mag. B **77** 1331, (1998).
[50] E. Koscielny-Bunde, A. Bunde, S. Havlin, H. E. Roman, Y. Goldreich and H. J. Schellnhuber, Phys. Rev. Lett. **81** 729 (1998).
[51] R. Benzi, L. Biferale, S. Ciliberto, M.V. Struglia, and R. Tripiccione, Physica D **96**, 162 (1996).
[52] A. Bershadskii and K.R. Sreenivasan, Phys. Lett. A **319**, 21 (2003).
[53] S. Ichimaru, Statistical plasma physics: condensed plasma, Vol 1 (Reprint edition (Jan 23 2004)).
[54] R. Benzi, S. Ciliberto, R. Tripiccione, C. Baudet, F. Massaioli and S. Succi, Phys. Rev. E **48**, R29 - R32 (1993).
[55] F. Ghasemi, K. Kaviani, M. Sahimi, M.R. Rahimi Tabar, F. Taghavi, S. Sadeghi, and G. Bijani, Computing in Science and Engineering March/April 2006 (Vol. 8, No. 2) pp. 54 (2006).